

Self-Association of Linker Histone H5 and of Its Globular Domain: Evidence for Specific Self-Contacts[†]

George John Carter[‡] and Kensal van Holde*

Department of Biochemistry and Biophysics, Oregon State University, Corvallis, Oregon 97331-7305

Received March 30, 1998; Revised Manuscript Received July 21, 1998

ABSTRACT: The ability of avian-specific linker histone H5, and the globular domains of H5 (GH5) and H1° (GH1°), to self-associate either free in solution or when bound to DNA was investigated. All three proteins underwent a salt-dependent increase in turbidity that may be indicative of nonspecific interactions. Dithiobis(succinimidyl propionate) cross-linking was used to measure specific contacts for both H5 and GH5 free in solution and bound to DNA. H5 and GH5 each became cross-linked in solution, with GH5 displaying divalent polymerization interactions, which suggests that two specific surfaces were involved in the assembly process. For GH5–DNA complexes, cross-linking appeared to be largely the consequence of aggregation, but under low concentrations of DSP, cross-linking GH5 was observed to assemble preferentially onto DNA before oligomerizing to form massive aggregates. Both linear and supercoiled DNA facilitated GH5 interactions compared to assembly in solution; differences in the distribution of cross-linked polymer sizes indicates that assembly is dependent on both the presence of DNA and the morphology of the DNA. Finally, on the basis of a technique referred to as quantitative proteolysis, GH5 assembly on DNA appears to involve specific protein–protein contacts involving the C terminus of one partner. Overall, the cumulative results reported here support the premise that linker histones assemble specifically both in solution and on DNA.

The main protein constituent of chromatin is comprised of a class of basic, structural proteins known as histones. Histones are further subdivided into linker histones and the octamer complex, the latter consisting of two subunits each of histones H2A, H2B, H3, and H4 (1). Linker histones bind to the complex of octamer and associated nucleosomal DNA in a roughly 1:1 stoichiometry (2) and stabilize the resulting chromatosomes as assayed by resistance of 168 bp DNA to nuclease digestion (3). The exact location of linker histone binding in the chromatosomes is unclear, and may actually involve multiple sites (4, 5). Additionally, it is well established that the chromatin fiber exists between two extreme conformations: extended and compacted fibers. Extended fibers are observed at low salt concentrations, and were originally reported to be relatively planar structures 10 nm in width as observed by electron microscopy (EM) (6, 7). In similar studies at high salt concentrations, compacted fibers were observed and reported to be relatively homogeneous solenoidal structures with a diameter of about 30 nm (8). However, recent scanning force microscopy (SFM) indicates that chromatin is considerably more heterogeneous in structure than indicated earlier from EM (9, 10).

Chromatin which has been stripped of linker histones experiences condensation upon their reintroduction (11) or

as a result of an increase in ionic strength (12, 13). The basis for fiber compaction remains a matter of some debate, though protein–protein interactions may contribute significantly. Histone octamers (14), linker histones (15), and nucleosomes have all been reported to self-associate in solution (16, 17). Particularly intriguing is the finding that self-association of nucleosomes or small oligonucleosomes is greatly enhanced by the addition of linker histones (16, 18). This suggests that linker histones may act as tethers in joining separate nucleosomes.

To date, attempts to determine whether linker histones specifically self-interact in the absence of a DNA or chromatin substrate have led to conflicting results from different research groups (15, 19, 20). As a step toward better understanding the process of linker histone self-interactions, and helping to resolve the reported discrepancies, we have assayed for linker histone self-association through several biochemical and biophysical approaches. These included analysis of linker histone assembly on DNA substrates, which was found to be a complicated process involving not only cooperative DNA loading but also aggregation. A novel analysis is introduced (referred to as quantitative proteolysis) that was developed for the purpose of detecting specific protein–protein contacts. Results indicate that both H5 and GH5¹ clearly interact to allow cross-linking with DSP when free in solution. Furthermore, evidence that does not support the possibility that linker histones interact in a specific manner both on DNA and when free in solution is presented.

[†] Supported in part by National Institutes of Health Grant GM50276.

* Corresponding author. Phone: (541) 737-4155. Fax: (541) 737-0481. E-mail: vanholdk@ucs.orst.edu.

[‡] Current address: Department of Internal Medicine, Division of Rheumatology, 5520 MSRB I, 1150 W. Medical Center Dr., Ann Arbor, MI 48109.

MATERIALS AND METHODS

Expression and Purification of Recombinant Human GH1° and Avian GH5. The trypsin-resistant globular domain of human subtypes H1° (GH1°) was cloned into the *Nco*I restriction site of pET-15b (Novagen) (21) by PCR amplifying residues 26–96 of the human H1° gene that had been previously cloned into pBluescript II SK (+) (22). For the PCR, the forward primer was ACC ACC CCA TGG GGT ATT CAG ACC TGA TCG TG that when translated included Met followed by Gly and residues 26–31 of the native H1° protein; the reverse primer was CTT GGG CCA TGG TCA CTT GGC TAG CCG GA. Fifty nanograms of template DNA, 0.7 μ g of both forward and reverse primers, 2.5 units of Taq polymerase (Pharmacia), and each dNTP at 0.125 mM were combined in a reaction solution containing 100 mM Tris-HCl (pH 9.0), 15 mM MgCl₂, and 500 mM KCl. The first PCR cycle included a denaturation step at 94 °C for 5 min, a primer annealing step at 65 °C for 1 min, and an extension step at 72 °C for 1.5 min. Subsequent cycles used a shorter (1 min) denaturation step with the final cycle including a 10 min extension step. Significant amounts of PCR-produced insert were detected with 30 cycles. The insert was ligated, using T4 DNA ligase (New England Biolabs), into the *Nco*I site of pET-15B (Novagen) and transformed into competent BL21 *Escherichia coli* cells (Novagen). Cells were induced to express recombinant GH1° with the addition of 0.6 mM IPTG at an A_{600nm} of 0.35–0.6 followed by several hours of shaking at 37 °C in LB. Clones expressing large quantities of peptide migrating at the expected location of GH1° were isolated and stored in 20% glycerol. One of these clones was randomly selected for large scale expression and purification.

Expressed GH1° was purified from the *E. coli* extract with a procedure based on a previously published protocol (23). Cells were pelleted, resuspended, and then sonicated for 10 min in buffer containing 25 mM Tris-HCl (pH 7.8), 0.5 M NaCl, 0.2 mM EDTA, and 0.35 mM PMSF. Cellular debris was spun down for 30 min in an SS-34 rotor with the supernatant resuspended in buffer and brought to 0.38 mg/mL ammonium sulfate. After brief vortexing, the solution was placed on ice for 30 min and then centrifuged for 30 min at 12 000 rpm in an SS-34 rotor. The sample was then dialyzed into 100 mM NaCl, 10 mM Tris-HCl (pH 7.8), and 0.2 mM EDTA in a Spectrapore 3 apparatus (molecular weight cutoff of 3500) overnight. After dialysis, the sample was loaded onto a CM Sephadex C25 (Sigma) column (5 cm \times 2.7 cm) that had been extensively washed with 300 mM NaCl, 10 mM Tris-HCl (pH 7.8), and 0.2 mM EDTA. The protein was eluted off the column at 20 mL/h with a gradient starting with 50 mL of 300 mM NaCl, 10 mM Tris-

HCl (pH 7.8), 1 mM EDTA, and 0.1 mM PMSF and ending with 50 mL of 1 M NaCl, 10 mM Tris-HCl (pH 7.8), 1 mM EDTA, and 0.1 mM PMSF. The purified protein was stored frozen in water. Recombinant GH5 from GH5pLK (24) was purified in the same manner. The recombinant GH5 includes residues 24–97 of intact H5, whereas the “native” GH5 obtained by trypsinization reportedly contains residues 22–100 (25). Recombinant GH5 and GH1° were quantitated using the UV absorbance as measured by a Hewlett-Packard 8452A diode array spectrophotometer using an $\epsilon_{280\text{nm}}$ of 4100 M⁻¹ cm⁻¹ and an $\epsilon_{230\text{nm}}$ of 34 000 M⁻¹ cm⁻¹ for GH5 and an $\epsilon_{280\text{nm}}$ of 4000 M⁻¹ cm⁻¹ and an $\epsilon_{230\text{nm}}$ of 31 000 M⁻¹ cm⁻¹ for GH1° (26).

Isolation of Linker Histone H5 from Chicken Erythrocytes. Native H5 was purified from chicken blood using an original procedure described by Garcia-Ramirez et al. (27). Briefly, chicken nuclei were isolated by disrupting chicken erythrocyte cells in 10 mM Tris-HCl (pH 7.8), 0.4 mM EDTA, 120 mM KCl, 30 mM NaCl, 0.2% Nonident P-40, and 0.3 mM PMSF. Nuclei were hypotonically lysed in 0.2 mM EDTA and 0.1 mM PMSF, and linker histones were salt extracted by bringing the resulting chromatin “jelly” to 0.65 M NaCl. CM Sephadex C25 cation exchange chromatography was used to separate purified linker histone H5 from linker histone H1 and other contaminants by washing extracted linker proteins from the CM Sephadex C25 column with 800 mM NaCl, 10 mM Tris-HCl (pH 7.8), and 0.2 mM EDTA. H5 was subsequently eluted off the column in 1.6 M NaCl, 10 mM Tris-HCl (pH 7.8), 0.2 mM EDTA, and 0.1 mM PMSF, dialyzed extensively into water, and stored frozen. Concentrations of H5 were determined from the following extinction coefficients: $\epsilon_{280\text{nm}}$ = 3900 M⁻¹ cm⁻¹ and $\epsilon_{230\text{nm}}$ = 48 000 M⁻¹ cm⁻¹ (26).

Circular Dichroism of Purified Proteins. Protein samples, stored frozen in water, were thawed and centrifuged for 30 min in a tabletop centrifuge to pellet any precipitate. Using a Cary 15 spectrophotometer purged with nitrogen gas, protein samples were initially diluted in water to give an absorbance at 184 nm of <1 OD in a quartz glass cuvette with a 1 mm path length. The cuvette was immediately transferred to a JASCO 720 spectropolarimeter, also purged with nitrogen gas, and scanned from 184 to 260 nm at 1 nm intervals at 20 nm/min. When the effect of sodium phosphate (pH 7.2) was observed, samples were removed from the cuvette, and an appropriate volume of 100 mM sodium phosphate (pH 7.2) buffer was added dropwise with the solution being vigorously pipetted up and down after each drop. Sodium phosphate buffer was prepared as a 200 mM sodium phosphate stock solution by titrating 200 mM sodium phosphate dibasic (Na₂HPO₄) with a smaller volume of 200 mM sodium phosphate monobasic (NaH₂PO₄) until a pH of 7.2 was reached.

Preparation of DNA Substrates. A 22 bp oligonucleotide duplex was formed by annealing the sequence GTA GTA ACG GAA GCC AGG TAT T to its complementary strand, and separately, a 42 bp oligonucleotide duplex with the sequence CCG GAA TTC GCA TCA TTG CCT TCG GTC CAT AAA GGA ATT CGG was annealed to its complementary strand. Salts associated with DNA synthesis [generated by a 380A DNA synthesizer (Applied Biosystems, Inc.)] were removed by G-50 Sephadex (Pharmacia) chromatography. The single-strand oligonucleotides were combined

¹ Abbreviations: BSA, bovine serum albumin; CD, circular dichroism; CM, carboxymethyl; dNTP, deoxyribonucleic acid triphosphate; DSP, dithiobis(succinimidyl propionate); EDTA, ethylenediaminetetraacetic acid disodium salt; GH1°, globular domain of human linker histone H1°; GH5, globular domain of chicken linker histone H5; IPTG, isopropyl β -D-thiogalactopyranoside; LB, Luria-Bertani bacterial growth media; PAGE, polyacrylamide gel electrophoresis; PCR, polymerase chain reaction; PMSF, phenylmethanesulfonyl fluoride; pPol208-12, twelve tandem copies of a 208 bp fragment from the 5S RNA gene of *Lytechinus variegatus* cloned into pUC19; SDS, sodium dodecyl sulfate; TCA, trichloroacetic acid; Tris-HCl, tris(hydroxymethyl)aminomethane hydrochloride.

in roughly equimolar proportions in 10 mM NaCl and 0.2 mM EDTA, and samples were heated to 90 °C in a heating block for 10 min and then cooled slowly back to room temperature at the rate of the cooling heating block. DNA concentrations were estimated by UV absorbance spectroscopy with an $\epsilon_{260\text{nm}}$ of $20 \mu\text{g}^{-1} \text{mL cm}^{-1}$.

Plasmid pPol208-12 (28) was isolated from DH5 α *E. coli* cells using the alkaline lysis procedure (29) and digested with *Hha*I (New England Biolabs) following the methods outlined by the manufacturer. The product of digestion consisted of the 208-12 insert, more than 2600 bp in length, as well as up to 16 smaller fragments, less than 400 bp in length, from *Hha*I cleavages of pUC19.

Salt-Induced Turbidity Analysis of GH5, GH1 $^{\circ}$, and H5. An aliquot of concentrated protein stock was diluted with water, and the absorbance of the sample was measured at 420 nm ($A_{420\text{nm}}$); we will refer to this absorbance as turbidity. If $A_{420\text{nm}} > 0.02$, the sample was centrifuged for 30 min at 13 000 rpm and 4 °C in a tabletop microcentrifuge to remove aggregates. Starting protein sample concentrations were as follows: (a) 0.27 mg/mL GH5, (b) 0.27 mg/mL GH1 $^{\circ}$, (c) 0.85 mg/mL H5, and (d) 2 mg/mL bovine serum albumin (BSA) (Sigma). Samples were then brought to 1 mM sodium phosphate (pH 7.2) by adding 100 mM sodium phosphate (pH 7.2), dropwise, followed by vigorously pipeting the solution up and down. $A_{420\text{nm}}$, or turbidity, was then measured to detect aggregation. To gauge the precipitability of the complexes, the sample was then centrifuged at 13 000 rpm and room temperature for several minutes to pellet salt-induced aggregates. The supernatant was then carefully decanted, and its $A_{420\text{nm}}$ was measured as before. After the absorbance of the supernatant was measured, the supernatant was used to resuspend the pelleted portion. The effect of NaCl on linker histone aggregation was analyzed by increasing the salt concentration in 50 mM NaCl increments by adding 5 M NaCl dropwise to samples and then by incubating the samples on ice for 15 min. After each increase in NaCl concentration, the $A_{420\text{nm}}$ was measured as described above.

Chemical Cross-Linking of GH5 and H5 in Solution. Unless otherwise stated, NaCl concentrations of histone solutions were adjusted in 1 mM sodium phosphate (pH 7.2) containing 0.2 mM EDTA by adding NaCl dropwise from a stock solution containing 5 M NaCl in 1 mM sodium phosphate (pH 7.2) and 0.2 mM EDTA to GH5 at 0.036 mM in 1 mM sodium phosphate (pH 7.2, 0.2 mM EDTA). Generally, salt concentrations were increased in 50 mM steps. Samples were incubated on ice for 10–15 min after each 50 mM NaCl increment, with these steps repeated until a final predetermined NaCl concentration was reached. Dithio-bis(succinimidyl propionate) (DSP) was prepared by making a 5 mg/mL stock solution in formamide following previously described protocols (15, 19, 20). Lyophilized DSP was suspended in formamide to a 20 \times stock and then the mixture added to the reaction solution to produce a final concentration of 0.1 mg/mL. The cross-linking reaction was conducted at room temperature with continuous shaking. Cross-linking was stopped by adding 2 \times SDS loading buffer [0.125 M Tris-HCl (pH 6.8), 4% SDS, 20% glycerol, and 0.04% bromophenol blue] and freezing the samples in liquid nitrogen. Samples were thawed immediately before analysis with 18% SDS–PAGE. Cross-linking with H5 at 0.018 mM was performed as described for GH5.

Chemical Cross-Linking of GH5 Assembled onto Linear DNA. Unless otherwise stated in the text, DNA at 0.05 mg/mL was incubated with GH5 in 10 mM NaCl, 10 mM Tris-HCl (pH 7.8), and 0.2 mM EDTA for 1 h at room temperature. Samples were then treated with 0.1 mg/mL DSP for 30 min with the reaction stopped with 0.1 M glycine. The reaction solution was brought to 28% v/v with ice cold TCA, precipitated on ice for 30 min, and centrifuged at 13 000 rpm for 1 h at 4 °C. After the supernatant was removed, ice cold 10 mM HCl-acetone was used to wash the pellet. The mixture was centrifuged for 30 min at 13 000 rpm using a tabletop centrifuge at 4 °C. All samples were resuspended in a common final volume of 10 mM Tris-HCl (pH 7.8) and 0.2 mM EDTA. For experiments in which the concentration-dependent effects of GH5 on cross-linked polymer distribution were investigated, reaction volumes were made inversely proportional to the GH5:DNA ratio and ranged from less than 100 μL for 140% GH5:DNA (w/w) to >1 mL for samples at 10% GH5:DNA (w/w) where noted. GH5 self-cross-linking on DNA was alternatively analyzed by SDS–PAGE as it was in the study of GH5 cross-linking free in solution.

Quantitative Proteolysis of GH5. GH5 at 0.04 mg/mL was incubated with the 22 bp oligonucleotide at 100% w/w for 35 min at 4 °C in buffered solution containing 10 mM sodium phosphate (pH 7.2), 8 mM NaCl, and 0.2 mM EDTA. The sample was then cross-linked in 0.01 mg/mL DSP (or 0.001 mg/mL for GH5 bound to the 42 bp fragment) from a 20 \times stock solution for 2 h at room temperature with constant shaking. The reaction was “stopped” with 50 mM glycine by shaking for 5 min. Chymotrypsin frozen in 10 mM Tris-HCl (pH 7.8) was added to a concentration of 0.3 $\mu\text{g/mL}$ from a 20 \times stock solution and the mixture incubated at room temperature for different amounts of time. Proteolysis was stopped with 1 mM PMSF, followed by the addition of 2 \times SDS loading buffer and freezing the resulting solution in liquid nitrogen. Products were analyzed by SDS–PAGE (18% polyacrylamide, 30:0.8 acrylamide:bi-sacrylamide). Similarly, GH5 at 0.04 mg/mL, free in solution, was cross-linked and proteolyzed with chymotrypsin, but with the following exception. DSP at 0.001 mg/mL was added to GH5 without preincubation.

Analysis with SDS–PAGE. SDS–polyacrylamide gels were constructed on the basis of the work of Laemmli (30). Gels were silver stained by a diamine silver staining protocol (31) that included the following steps: fixing the gels in 45% methanol/9% acetic acid for several hours, washing the gel for about 1 day with repeated changes of water, and then staining and developing the gel. For Coomassie staining, the gel was stained for 30 min in 45% methanol (v/v), 9% acetic acid, and 0.25% (w/v) Coomassie G-250 and then destained in 7.5% acetic acid and 5% methanol with a kimwipe to absorb Coomassie from the gel. Gels were quantitated by analyzing the scans of photographs with NIH Image (version 1.57) (32).

RESULTS

Characterization of Purified Proteins. H5, GH5, and GH1 $^{\circ}$ were all purified to greater than 95% homogeneity as determined from silver stain SDS–polyacrylamide gels (data not shown). To ensure that the protein properly folded under

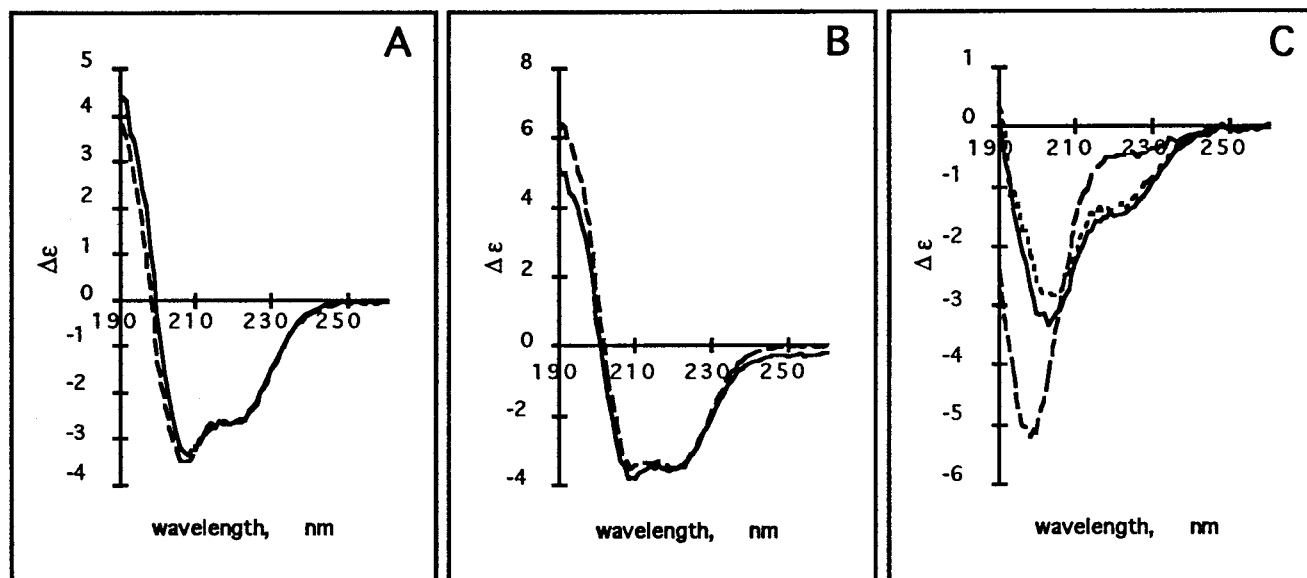


FIGURE 1: Circular dichroism of linker histone proteins, and the effect of PO_4^{3-} . The CD spectra of (A) recombinant GH1°, (B) recombinant GH5, and (C) native H5 were measured using a Jasco 720 spectropolarimeter. Samples were measured in water (---), in 1 mM sodium phosphate (pH 7.2) (---), and in 10 mM sodium phosphate (—). $\Delta\epsilon$ ($\text{cm}^{-1} \text{mg}^{-1} \text{mL}$) is shown as a function of wavelength (nm).

the conditions of isolation outlined in Materials and Methods, the secondary structure of each linker histone was analyzed using circular dichroism (CD). The proteins differed in their relative proportion of secondary elements, and in their response to sodium phosphate (pH 7.2). While GH1° (Figure 1A) and GH5 (Figure 1B) were relatively unaffected by the presence of sodium phosphate (pH 7.2), H5 underwent considerable restructuring which presumably involved folding of the tail domains (Figure 1C). The presence of 1 mM sodium phosphate (pH 7.2) appeared to be sufficient for H5 folding as the CD profile changed relatively little at 10 mM sodium phosphate (pH 7.2). The results support previous reports of linker histone tail folding either in the presence of phosphate ion (33, 34) or when H5 binds to DNA (33–35).

The general form of the CD spectra, the folding behavior in phosphates, and the estimated % α -helical residues indicate that the purified proteins were properly folded after the isolation procedure. The relative proportion of α -helical residues was estimated using the approximate relationship % α -helix = $(\Delta\epsilon_{220\text{nm}} - 0.25)/0.105$ (34). For GH5, the secondary structure was relatively unaffected by sodium phosphate buffer as the % α -helix remained constant from 36 to 35% with an increase from 0 to 10 mM sodium phosphate (pH 7.2). Under the same conditions, GH1° also was unaffected, changing negligibly from 27.5 to 27.6%. H5, in contrast, experienced a considerable change in the % α -helix with 7.37, 15.6, and 14.8% in water, 1 mM sodium phosphate (pH 7.2), and 10 mM sodium phosphate (pH 7.2), respectively. For GH5, these data indicate that 26 residues were involved in α -helices which compares to 33 residues reported for GH5 prepared from native H5 on the basis of CD measurements (15). However, these two preparations should not be directly comparable because of their differences in chain length (see above). Other measures include a value of 32 residues from the NMR of GH5 (36) and 39 residues for crystallized, recombinant GH5 (37). Low values for % α -helices have been noted before using circular dichroism (15). In addition, GH1° appeared to have considerably less

α -helix with 20 residues, despite its high degree of homology to GH5. On the other hand, our results for native H5 appear to be nearly the same as those reported by Clark et al. (34), with 16 and 17%, respectively.

Salt-Induced Turbidity of H5, GH1°, and GH5 Solutions. Salt-induced turbidity has previously been used to detect DNA–linker histone interaction in solution (38, 39). In those studies, it was reported that DNA–protein aggregation is a salt-dependent process with maximum turbidity occurring at around 0.25 M NaCl. As a comparison to these earlier studies, and to determine whether linker histone-related peptides can under any circumstances aggregate in the absence of DNA to form large complexes, we examined the effect of NaCl on the turbidity of solutions of linker histones.

Results indicate that above about 0.25 M NaCl, GH1°, GH5, and H5 all experienced a salt-dependent increase in turbidity, with all proteins displaying nearly equivalent responses (Figure 2A). Each histone produced considerably more salt-induced turbidity than bovine serum albumin in this salt range. At lower salt concentrations, the low turbidity was not significantly greater than that of BSA. Interestingly, each linker protein exhibited similar inflection points at about 0.45 and 0.85 M NaCl, at which points the turbidity increased abruptly. The pelleting behavior of the aggregates was also investigated by comparing the $A_{420\text{nm}}$ before pelleting to the $A_{420\text{nm}}$ of the supernatant after centrifugation for several minutes at 13 000 rpm (Figure 2B). The H5 aggregate was far more resistant to pelleting than was either the GH5 or GH1° aggregate; only about 20% of the H5 aggregate was pelleted under these circumstances as compared to 60–90% of the GH5 or GH1° aggregates. The aggregation process appeared to be irreversible, for dilution reduced the concentration-normalized $A_{420\text{nm}}$ to the inverse of the dilution volume (data not shown).

In summary, the salt-dependent increase in turbidity indicates that the linker histone proteins themselves, without DNA, are capable of interacting to form large aggregates at high salt concentrations. The common inflection points, and roughly equivalent response to NaCl for H5, GH5, and GH1°,

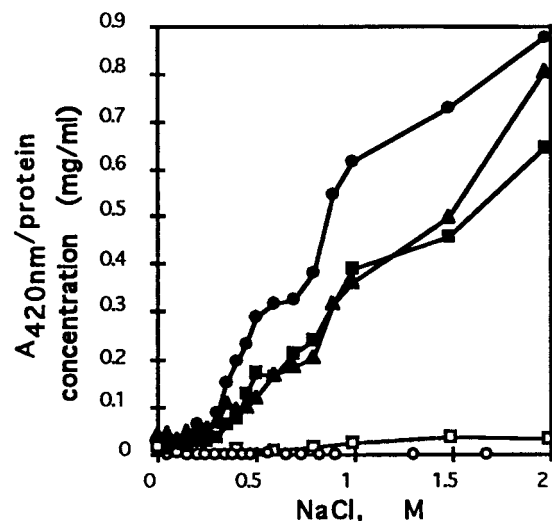


FIGURE 2: Salt-dependent turbidity analysis of linker histone proteins. Proteins were titrated to increasing ionic strengths by adding NaCl in 50 mM increments while in 1 mM sodium phosphate (pH 7.2) and 0.2 mM EDTA. Turbidity was measured by the absorbance at 420 nm ($A_{420\text{nm}}$), and all values are adjusted to reflect dilution by the addition of NaCl stock and normalized by the protein concentration. Samples included H5 (■), GH5 (●), GH1° (▲), serum albumin (□), and buffered solution (negative control) (○).

as well as the common stepwise increases in turbidity suggest that the proteins were interacting (and aggregating) in a similar fashion. What this actually represents from a protein interaction model is unclear. The aggregation process did not appear to be enhanced by the presence of the linker histone tails; rather, self-interaction of the globular domain appears to have been responsible for the effect as judged by the common response by all three proteins. The tail domains did however increase the ability of the H5 aggregate to resist sedimentation (as compared to the globular domains), though it is uncertain whether the tail domains increased nucleoprotein complex solubility or remodeled the aggregate complex structure. It should be emphasized that the turbidity measurements give no indication of the fraction of the protein involved in the aggregate at any given salt concentration; rather, the results should be used for comparative purposes at different salt concentrations. However, light scattering did indicate that proteins were interacting, though it will require other techniques to better characterize this self-association.

Cross-Linking of GH5 and H5 Free in Solution. A more direct and quantitative approach to the question of self-association can be provided by chemical cross-linking. Extensive cross-linking in solution is taken to be indicative of specific interactions, since random collisions are expected to produce a minimal amount of cross-linking (15). DSP was used as the cross-linking molecule; it has a 1.2 nm cross-linking length, and reacts primarily with ϵ -amines of lysine residues. In recent years, three separate research groups have used DSP in attempts to determine whether GH5 self-associates in solution (15, 19, 20). However, the data in the literature are contradictory; only Maman et al. (15) were able to successfully cross-link GH5, reporting a K_a of $4.8 \times 10^3 \text{ M}^{-1}$. This value, although suspect because it was measured in a nonequilibrium cross-linking system, indicates that the association if real is weak.

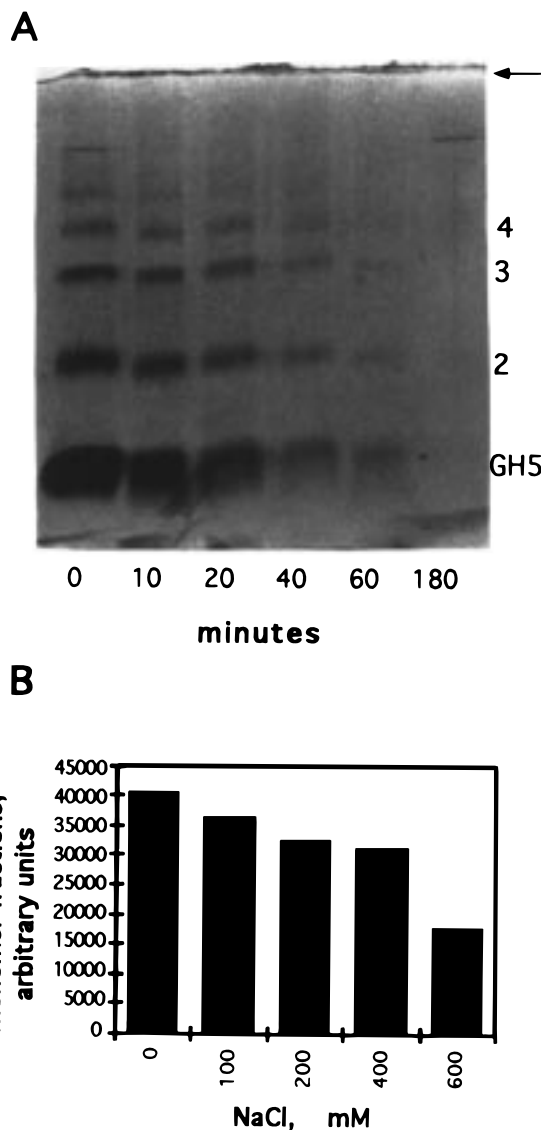


FIGURE 3: Cross-linking GH5 free in solution with DSP. (A) Time course of GH5 cross-linking at $4.9 \mu\text{M}$ (0.04 mg/mL) at room temperature in 10 mM NaCl, 10 mM sodium phosphate (pH 7.2), and 0.2 mM EDTA. Samples were separated on an 18% Laemmli gel and silver stained. The arrow denotes location of the stacking gel-separating gel boundary. The numbers on the right side of the gel refer to the number of chemically cross-linked GH5 molecules in each oligomer. The relatively small amount of polymerization observed at 0 min (<10% total mass) is due to cross-linking that occurred during the 2–3 min process of freezing and thawing the sample before SDS-PAGE separation (see Materials and Methods). Virtually all GH5 existed as monomer-sized protein in samples not cross-linked (data not shown). (B) The effect of salt on cross-linking efficiency was measured by the fraction of the GH5 monomer left un-cross-linked in 1 mM sodium phosphate (pH 7.2), 0.2 mM EDTA, 0.1 mg/mL DSP, and various salt concentrations as scanned from a representative gel at 30 min.

Our experiments unequivocally demonstrate cross-linking of both GH5 and H5 in solution. The process is rapid, as polymers of various sizes were observed by SDS-PAGE within a few minutes of cross-linking, and nearly all GH5 became cross-linked into large aggregate complexes within a couple of hours. Figure 3A illustrates the cross-linking of GH5 at 0.04 mg/mL for various lengths of time in low-salt buffer. Coomassie staining of the gel revealed minimal cross-linking of the sample at early time points, but the more sensitive silver staining showed complexing even at the

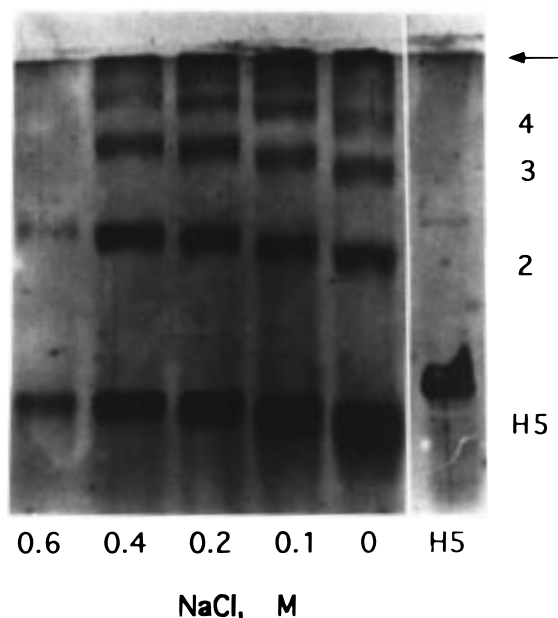


FIGURE 4: Cross-linking H5 free in solution with DSP at varying salt concentrations. H5 at 0.018 mM (0.38 mg/mL) was cross-linked for 30 min at room temperature with 0.1 mg/mL DSP with various NaCl concentrations, 1 mM sodium phosphate (pH 7.2), and 0.2 mM EDTA. Samples were separated on a 12% Laemmli gel and silver stained. The arrow denotes the location of stacking gel-separating gel boundary.

“zero” time point. Therefore, oligomerization must have occurred in the time required to mix and freeze samples (zero time, Figure 3A), and all material became too large to enter the gel by 3 h.

To measure the effect of NaCl on the cross-linking rate, GH5 at 0.036 mM (0.29 mg/mL) was incrementally increased in 50 mM NaCl steps to salt concentrations between 0 and 600 mM NaCl in 1 mM sodium phosphate buffer and 0.2 mM EDTA and then cross-linked with 0.1 mg/mL DSP for 30 min (Materials and Methods). The cross-linking rate, as measured by monomer disappearance in 30 min, increased as a function of the NaCl concentration, with samples in 600 mM NaCl cross-linking about twice as fast as those in 0 mM NaCl (Figure 3B). Initially, 50 mM glycine was used to stop the cross-linking reaction, but appeared only to slow the reaction as storage on ice overnight led to the production of massive aggregates (data not shown). Because of this, samples were instead frozen with liquid nitrogen in 2× SDS loading buffer, which appeared to be quite effective in stopping the reaction.

In a comparable study, H5 at 0.018 mM was cross-linked in 0.1 mg/mL DSP as described for GH5. Previously, H5 was reported to cross-link in 1% formaldehyde into polymers up to trimers (40), but Clark and Thomas (41) were unable to detect cross-linking using DSP. We found that H5 cross-linked into polymers extending from monomers to complexes too large to enter the 12% polyacrylamide gel (Figure 4). After the cross-linking reaction, the remaining monomeric H5 showed a considerable increase in electrophoretic mobility. This was likely due in part to the neutralization of lysine amino groups in the histone tails, but may have also included internal cross-linking which compacted the molecule. Supporting the latter explanation is the observation that with addition of 1 mM sodium phosphate (pH 7.2) (which induces tail domain folding), the electrophoretic mobility increased

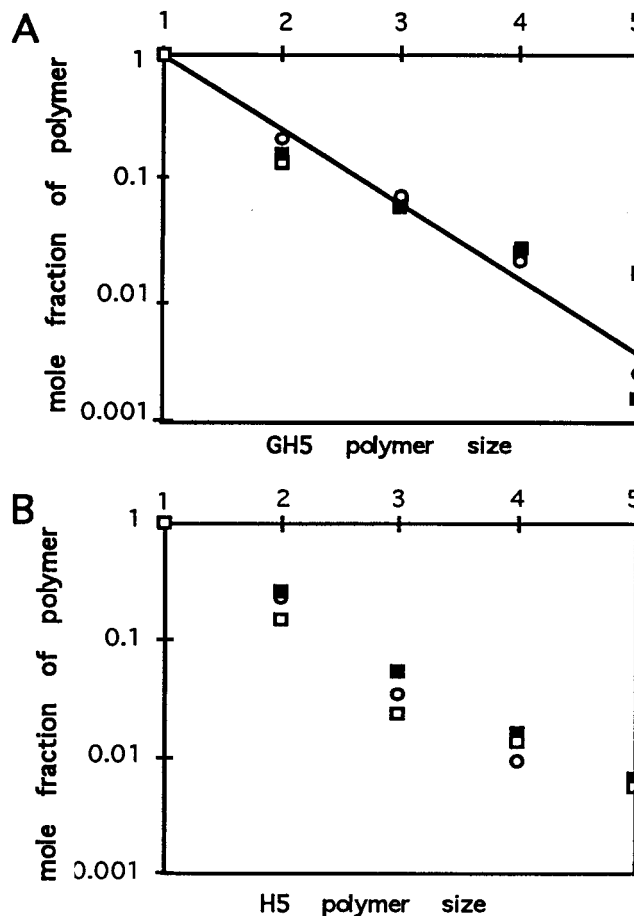


FIGURE 5: Semilogarithmic plot of the GH5 and H5 DSP-cross-linked polymer distribution. (A) A graph of the log of the relative molar amount of each GH5 polymer DSP-cross-linked free in solution as a function of polymer size at several different times of cross-linking. Conditions were like those described in the legend of Figure 3A: cross-linking for 10 min (○), cross-linking for 20 min (■), and cross-linking for 40 min (□). (B) A graph of the log of the relative molar amount of each H5 polymer DSP-cross-linked free in solution for 30 min as a function of polymer size at three NaCl concentrations: 200 mM NaCl, 1 mM sodium phosphate (pH 7.2), and 0.2 mM EDTA (■), 100 mM NaCl, 1 mM sodium phosphate (pH 7.2), and 0.2 mM EDTA (□), and water (○). The relative molar amount for each polymer was calculated by dividing the mass of the respective polymer by the mass of the monomer product (at the indicated time) as determined from a silver-stained gel. This value was then converted to a molar value by dividing the relative mass of each polymer by the number of proteins found in that particular polymer complex (for a dimer this value is two, and for a trimer this value is three).

even more, suggesting that lysines in the tails made close enough contact to cross-link, reducing the effective size of the protein. Like GH5, all H5 molecules eventually became cross-linked with DSP, producing protein complexes too large to enter the 5% polyacrylamide stacking gel, with no detectable monomers remaining.

A plot of the logarithm of the relative molar proportion for each GH5 polymer (relative to the amount of GH5 monomer product) as a function of polymer size revealed a roughly linear relationship (Figure 5A). According to Flory (42), such a relationship is a consequence of “divalency” in which monomers form linear filaments via a single, repeating interaction interface. This is in contrast to more complicated multiple contacts that lead to “branching”. For such a linear polymerization,

$$\ln\left(\frac{N_x}{N_1}\right) = (x - 1) \ln p \quad (1)$$

where N_x is the molar amount of polymer of size x , N_1 is the molar amount of monomer, and p is the probability that any one of the reactive surfaces, chosen at random, has reacted. The value of p for GH5 cross-linked in 10 mM NaCl, 10 mM sodium phosphate (pH 7.2), and 0.2 mM EDTA showed some variation with the time of cross-linking. Although the data are limited, p appears to increase with the time of cross-linking, as might be expected. At longer times of cross-linking, some deviation from linearity is seen (Figure 5A). This is expected if extensive cross-linking produces some branched aggregates, and suggests that limited reaction at alternative sites also occurs.

In contrast to the GH5 data, a plot of the log of the relative molar fraction for each polymer as a function of polymer size for H5 appeared to be nonlinear under all conditions (Figure 5B). The nonlinearity could be explained if H5 polymers assembled with a valency of >2 (42); larger, branched aggregates have more opportunities to add units, and thus, larger aggregate formation is more abundant than linear polymerization at comparable levels of reaction. Quite possibly, the long, flexible C-terminal tail domains of H5 provide additional interaction sites not present in the compact, globular GH5.

Importance of Protein–Protein Contacts in GH5 Assembly onto Small Oligonucleotides. As a direct corollary to the solution studies, DSP cross-linking was used to measure the frequency and distribution of GH5 self-interactions on DNA substrates. The propensity for GH5 to self-associate on DNA is suggested by both its cooperativity in binding (43) and electron micrographs that show clustering of the molecules when they are bound to DNA (30, 44). To better understand the importance of protein–protein contacts, GH5 cross-linked free in solution (Figure 6A) was compared to the assembly onto two different sized oligonucleotides. GH5 at 0.04 mg/mL was bound to either a 22 bp oligonucleotide (Figure 6B) or a 42 bp oligonucleotide (Figure 6C) at 100% GH5:DNA (w/w). The histone mixtures were incubated in 8 mM NaCl, 10 mM sodium phosphate buffer, and 0.2 mM EDTA for 35 min and then reacted with DSP for 2 h at room temperature. Under these conditions, 0.001 mg/mL DSP was found to be optimal for GH5 cross-linking when it was bound to the 42 bp oligonucleotide, and 0.01 mg/mL was found to be optimal for GH5 cross-linking when it was bound to the 22 bp oligonucleotide. Under the above-described reaction conditions, greater DSP concentrations led to over-cross-linking in which no clear preferred number of cross-linked molecules was observed (data not shown). As a comparison, GH5 free in solution at 0.036 mM was cross-linked in 0.1 mg/mL DSP for 30 min in 400 mM NaCl, 1 mM sodium phosphate (pH 7.2), and 0.1 mM EDTA. It is apparent from Figure 6 that the preferred size of cross-linked GH5 molecules was dependent on both the presence and size of the oligonucleotide. While GH5 cross-linked free in solution displayed a molar logarithmic distribution (see the previous section), the histograms for GH5 DSP-cross-linked on the 22 and 42 bp oligonucleotides showed a strong preference for cross-linking to produce complexes with two and three GH5 molecules, respectively. However, there was also

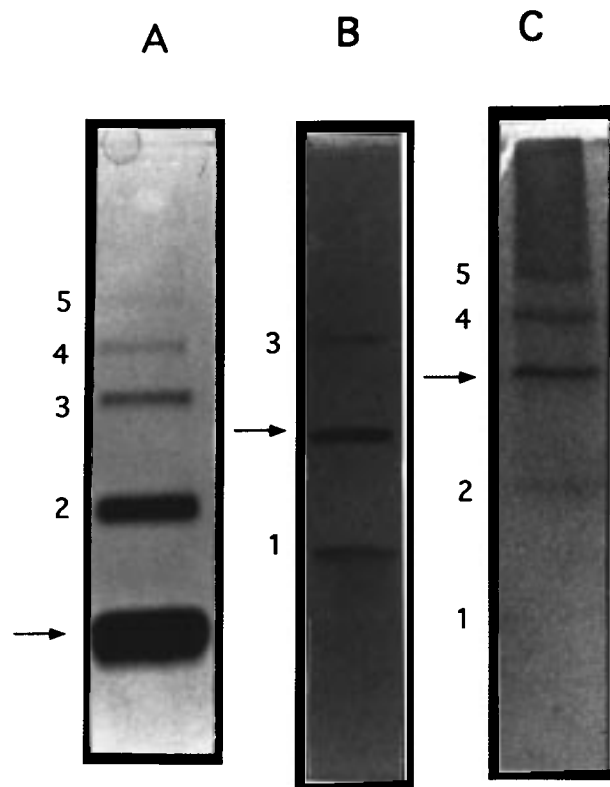


FIGURE 6: GH5 molecules preferentially bound to DNA as a function of oligonucleotide size. (A) GH5 at 0.036 mM (0.29 mg/mL) was cross-linked free in 1 mM sodium phosphate (pH 7.2), 0.2 mM EDTA, and 500 mM NaCl with 0.1 mg/mL DSP for 35 min. (B) GH5 was cross-linked onto a 22 bp oligonucleotide at 0.04 mg/mL [100% GH5:DNA (w/w)] in 0.01 mg/mL DSP in 8 mM NaCl, 0.2 mM EDTA, and 10 mM sodium phosphate buffer (pH 7.2) for 2 h. (C) GH5 was cross-linked onto a 42 bp oligonucleotide as described for the 22 bp oligonucleotide in panel B. Samples were treated with 2× SDS, frozen in liquid nitrogen for storage, and applied directly to an 18% SDS–polyacrylamide gel. Arrows point to the single most populous GH5 oligomer (mass amount), in each case.

extensive interaction between separate GH5–DNA complexes (particularly for the 42 bp–histone complexes) as reflected by the formation of protein oligomer bands extending to the well of the gel (Figure 6C). Presumably, these larger complexes resulted from cross-linking between GH5 molecules bound to different DNA oligomers.

If the number of base pairs of the oligonucleotide is divided by the mode of the number of cross-linked GH5 molecules, the binding site size can be estimated. A binding site size of 11 bp/GH5 was calculated in this way from the data for the 22 bp DNA, and 14 bp/GH5 from the data for the 42 bp DNA. These values are experimentally indistinguishable, and are also consistent with the value of 10 bp/GH5 previously estimated by Thomas et al. (19) in a less direct fashion. The calculation does not consider the possibility of free end effects (20, 44) or the possibility that only part of a GH5 molecule binds the end.

In summary, a core group of closely associated, DNA-bound proteins were cross-linked together onto the oligonucleotides at low DSP concentrations. The clear dependence of the preferred number of cross-linked molecules on the size of the oligonucleotide suggests that protein–protein contacts were due to protein assembly on individual DNA fragments. Therefore, these results support the argument that

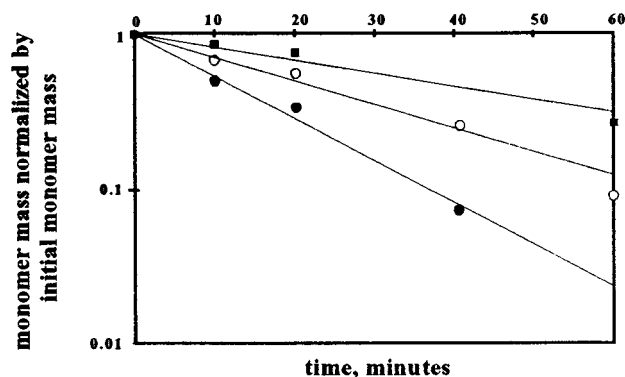


FIGURE 7: Influence of the type of DNA substrate (or lack of substrate) on the kinetics of GH5 self-interaction. A time course of GH5 cross-linking was measured by plotting the logarithm of the mass of un-cross-linked monomers (normalized to the initial monomer mass) as a function of time. GH5 at 0.04 mg/mL was incubated with either pUC19 plasmid DNA (100% GH5:DNA w/w) (○) or a 42 bp oligonucleotide (100% GH5:DNA w/w) (●) in 10 mM sodium phosphate (pH 7.2) and 0.2 mM EDTA for around 35 min at 4 °C before cross-linking in 0.1 mg/mL DSP at room temperature. GH5 was DSP-cross-linked in the absence of DNA under the above-mentioned conditions (with the addition of 10 mM NaCl) (■). Samples were treated with 2× SDS, frozen in liquid nitrogen for storage, and applied directly to an 18% SDS–polyacrylamide gel. A “best-fit” line representing the remaining, un-cross-linked GH5 monomers was generated using linear regression of the data points of silver-stained gels (Microsoft Excel 5.0).

contacts between GH5 molecules bound to the same DNA molecule were preferred over interactions between GH5 molecules bound to separate DNA complexes, though these contacts must also have occurred after prolonged cross-linking to give rise to nucleoprotein aggregation.

Kinetics of GH5 Association Depend on the DNA Substrate. The influence of DNA substrate on the rate of GH5 association was also examined using DSP cross-linking. GH5 was cross-linked for various periods of time in the presence and absence of a 42 bp oligonucleotide. In comparison, a parallel study was conducted with supercoiled pUC19 plasmid DNA (2600 bp in size). For DNA-dependent cross-linking, GH5 and DNA both at 0.04 mg/mL were preincubated on ice for 35 min in buffered solution containing 10 mM sodium phosphate (pH 7.2) and 0.2 mM EDTA before adding DSP to 0.1 mg/mL. For solution cross-linking, GH5 at 4.9 μ M (0.04 mg/mL) was cross-linked under the same conditions but with 10 mM NaCl added to the reaction solution. At various time points, DSP reactions were stopped with the addition of 2× SDS loading buffer, and by freezing the contents of the reaction mixture in liquid nitrogen.

On the basis of the rate of disappearance of GH5 monomers into large cross-linked complexes, the presence of DNA clearly influenced the cross-linking rate. The data could be fitted to a first-order process, as shown in Figure 7. GH5 that was bound to the 42 bp oligonucleotide cross-linked faster than GH5 free in solution with a rate constant (k) of 0.062 min^{-1} for the former and 0.023 min^{-1} for the latter. The much larger plasmid DNA also led to increased GH5 contact frequency compared to that for the GH5 cross-linking free in solution with a cross-linking rate k of 0.037 M min^{-1} .

Effect of NaCl and the Protein:DNA Ratio on GH5–GH5 Contacts. It has been reported that the frequency of protein–protein contacts increases together with cooperativity in

linker histone binding to DNA (41). Consistent with this idea, linker histone H1 undergoes increased DSP-dependent cross-linking with increases in NaCl concentration (44), as well as with increased protein:DNA input ratios. In contrast, H5 self-cross-linking on a DNA substrate is insensitive to salt or protein:DNA ratio (41). On this basis, we should expect that contact between H5 molecules on DNA would be unaffected by either of these parameters. It was therefore interesting to observe how the GH5 cross-linking distribution was affected by changes in protein concentration and salt concentration, especially in view of a report indicating that GH5 cooperativity is similar to that of H5 (19).

GH5 was bound to a mixture of linear DNA fragments obtained by *Hha*I-cut pPol208-12. The fragment sizes ranged from 2600 bp to small fragments of less than 400 bp. Ratios of GH5:DNA between 10 and 140% (w/w), as well as NaCl concentrations of 10 and 100 mM, were used to elucidate the effects of protein concentration and NaCl on protein–protein contacts. The pattern of histone cross-linking appeared to be independent of the GH5:DNA ratio, as a change from 10 to 140% produced a nearly identical distribution of polymer sizes at all GH5:DNA ratios analyzed (Figure 8A). This is in contrast to the effect of NaCl on the polymer distribution. Samples at 140% GH5:DNA (w/w) showed a considerable increase in the number of cross-linkable protein–protein contacts with increasing salt concentrations (Figure 8B). The difference was considerably more dramatic for polymers larger than a dimer, with GH5 bound to DNA in 100 mM NaCl cross-linking more extensively than in 10 mM NaCl at the same protein:DNA ratio.

While the independence of GH5 cross-linking on the GH5:DNA input ratio appears to mimic previously reported H5 studies, the salt concentration dependency of GH5 cross-linking came as a surprise, considering that results from Clark and Thomas (41) and Draves et al. (20) would predict that GH5 and H5 should display a similar salt concentration independence in DNA binding and cooperativity. In explaining the apparent inconsistency between cross-linking results presented here and previous reports, we must emphasize that oligomerization and aggregation of GH5–DNA complexes result in an increase in the number of GH5 contacts between molecules on separate DNAs (see above), and aggregation has been reported to increase with salt concentration (26, 46). In view of all the data, it seems most likely that the increased cross-linking observed at high salt concentrations arises from the aggregation of DNA–linker histone complexes, which allows for closer or more permanent protein–protein contacts.

Effect of the Type of DNA Substrate on GH5–GH5 Contacts. It is well established that linker histones interact differently with linear DNA and supercoiled DNA. First, linker histones prefer to bind supercoiled DNA instead of linear DNA (47) with binding affinity increasing with superhelicity (48, 49). Second, linker histones are distributed relatively evenly among the population of supercoiled DNA (50, 51), whereas for linear DNA, linker histones cooperatively bind to some DNA fragments while leaving other DNA fragments completely unbound (19). Third, linker histones more readily associate with and aggregate linear DNA than supercoiled DNA (46). As a way of determining if GH5 also assembles differently on linear and supercoiled DNAs,

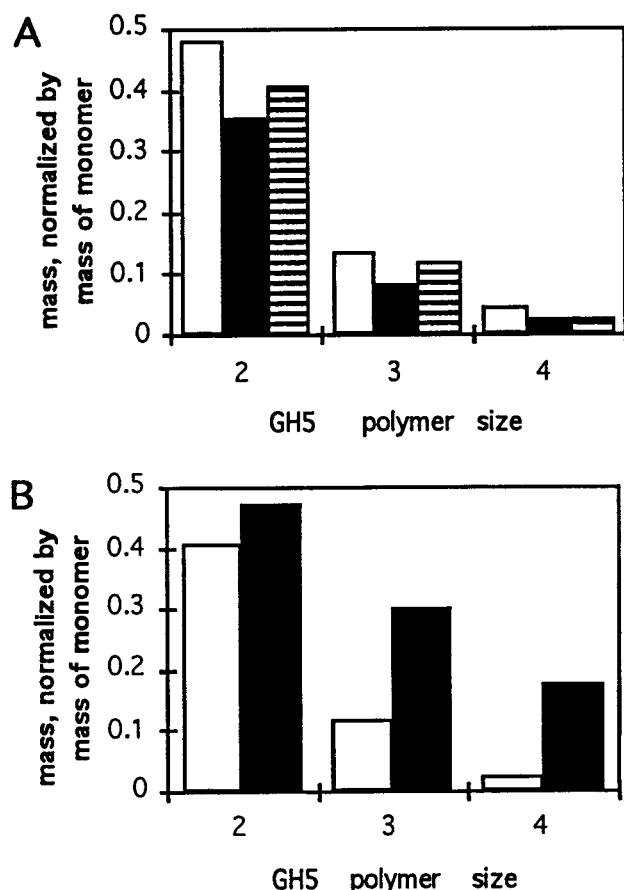


FIGURE 8: Effect of the GH5:DNA ratio and ionic strength on the polymer distribution of GH5 cross-linked onto DNA. (A) Comparison of the distribution of GH5 polymers as a function of GH5:DNA (w/w) ratios. GH5 was incubated with 0.05 mg/mL *HhaI*-cut pPol208-12 in 10 mM NaCl, 1 mM sodium phosphate (pH 7.2), and 0.2 mM EDTA, cross-linked with 0.1 mg/mL DSP for 30 min, and precipitated with 28% TCA (Materials and Methods). Samples include 10% GH5:DNA (w/w) (white bar), 50% GH5:DNA (w/w) (black bar), and 140% GH5:DNA (w/w) (striped bar). (B) Comparison of the distribution of GH5 polymers as a function of either 10 (white bar) or 100 mM NaCl (black bar) at 140% GH5:DNA (w/w) under the conditions described for panel A.

DSP-facilitated cross-linking was used to measure molecular contact frequency.

In an examination of the influence of DNA topology on GH5 association, and cross-linking, GH5 was cross-linked, separately, onto a 42 bp oligonucleotide, onto *HhaI*-cut pPol208-12 DNA, onto a supercoiled pUC19 plasmid, and free in solution. Time points were chosen for comparison where roughly the same amount of cross-linking had occurred, as judged by the disappearance of GH5 monomers (Figure 7). GH5 bound to linear DNA (both the 42 bp oligonucleotide and *HhaI*-cut pPol208-12 DNA) clearly formed a larger proportion of high-molecular weight GH5 homopolymers than did GH5 cross-linked free in solution (Figure 9). GH5 also cross-linked on supercoiled DNA in a manner different from that of other DNA substrates. GH5 which was cross-linked on supercoiled DNA showed a strong propensity to form only small GH5 oligomers (trimers and smaller), or formed complexes too large to enter the running gel (data not shown). In contrast, GH5 cross-linked while bound to linear DNA or cross-linked while free in solution appeared to form a continuous, logarithmic distribution, similar to results presented in Figure 5. Furthermore, the

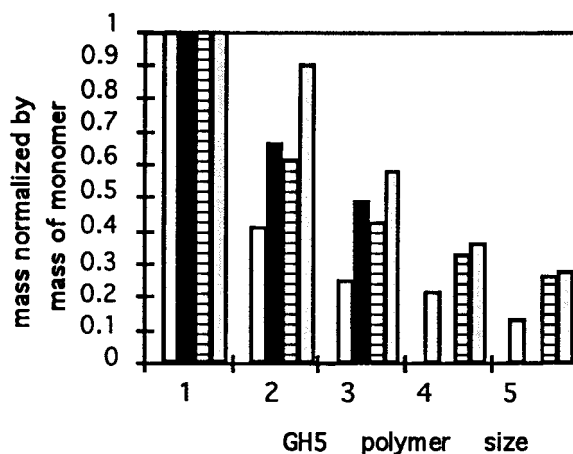


FIGURE 9: Effect of DNA substrate on the distribution of DSP-cross-linked polymers. The distribution of DSP-cross-linked polymers was measured for a number of samples. Reaction conditions were as follows. GH5 at 0.036 M (0.29 mg/mL) was cross-linked in 10 mM NaCl and 10 mM sodium phosphate (pH 7.2) as described in Figure 7, at the 20 min time point (white bar). GH5 at 0.04 mg/mL was cross-linked onto supercoiled DNA [100% GH5:DNA (w/w)] as described in Figure 7 in 10 mM sodium phosphate buffer (pH 7.2), at the 40 min time point (black bar). GH5 at 0.04 mg/mL was cross-linked onto a 42 bp oligonucleotide [100% GH5:DNA (w/w)] as described in Figure 7 in 10 mM sodium phosphate (pH 7.2), at the 20 min time point (striped bar). GH5 cross-linked onto *HhaI*-cut pPol208-12 at 140% GH5:DNA (w/w) as described in Figure 8 in 10 mM NaCl and 1 mM sodium phosphate (pH 7.2), at the 30 min time point (speckled bar). All samples were treated with DSP at room temperature. Since the cross-linking rates varied somewhat depending on the sample conditions, time points were chosen to give roughly comparable levels of disappearance of the GH5 monomer.

length of linear DNA (42 vs 2600 bp) did not appear to markedly influence the polymer distribution at these high levels of cross-linking, suggesting that oligomerization between separate small DNA-protein complexes may mimic GH5 assembly on long linear DNA.

Characterizing Cross-Linked GH5 Assemblies by Quantitative Proteolysis. To elucidate the organization of cross-linked GH5 complexes and to search for evidence for specific contacts in cross-linking, a technique involving cross-linking followed by proteolysis was developed. This assay is referred to as quantitative proteolysis. In this method, GH5 was first cross-linked with DSP and then proteolyzed with chymotrypsin, which cleaves preferentially at a single site in GH5, to the carboxyl side of Phe 93. Information on filament structure was then determined on the basis of the size distribution of the proteolyzed peptide products, hence the name quantitative proteolysis. The technique can best be used for characterizing indefinite filaments comprised of proteins that self-interact via only two surfaces (26).

Quantitative proteolysis was used to elucidate the cross-linked organization of GH5 assembled on oligonucleotides. GH5 at 0.04 mg/mL was mixed with a 22 bp oligonucleotide at 0.04 mg/mL in 10 mM sodium phosphate (pH 7.2) for 35 min on ice before being cross-linked with DSP for 2 h at 4 °C. After the cross-linking reaction was "quenched" in 50 mM glycine, the GH5-DNA sample was proteolyzed with chymotrypsin. It was found that samples at 0.01 mg/mL DSP produced the best results, since GH5-DNA complexes cross-linked at higher DSP concentrations seemed to be unaffected by chymotrypsin proteolysis (data not shown).

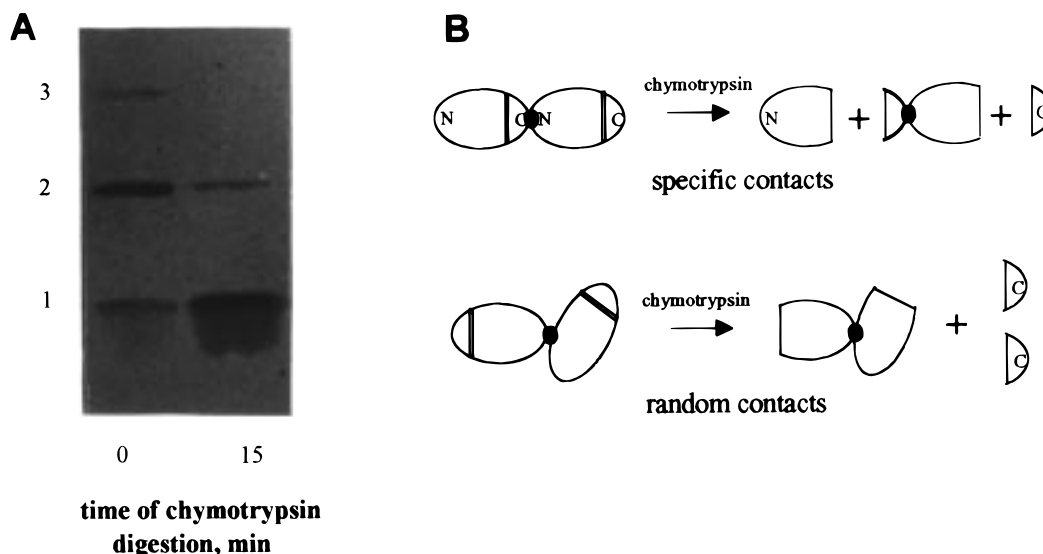


FIGURE 10: Determining DSP-cross-linked GH5 complex organization by quantitative proteolysis. (A) GH5 at 0.04 mg/mL was incubated with a 22 bp oligonucleotide at 100% (w/w) for 35 min in 8 mM NaCl, 10 mM sodium phosphate (pH 7.2), and 0.2 mM EDTA and treated with 0.01 mg/mL DSP for 2 h. Samples were brought to 50 mM glycine and then cleaved with 0.3 μ g/mL chymotrypsin at room temperature for 15 min. Virtually no cross-linked GH5 complexes larger than trimers were observed, even on silver-stained gels. (B) Models for possible assembly and quantitative proteolysis of GH5 molecules bound to a 22 bp oligonucleotide include random association or association based on specific contacts in which the C-terminal region of one molecule contacts a specific site of another molecule. Chymotrypsin cleavage of such a specific association results in the production of two peptides roughly the size of a monomer, as observed for the experiment depicted in panel A; small peptide four amino acids in size should also be produced, but would not be observable on these gels. Dots represent DSP cross-linking points that covalently attach two separate molecules, and double lines represent chymotrypsin cleavage sites.

Interestingly, at low concentrations, GH5 cross-linked primarily as a dimer with the dimer rapidly becoming reduced to mostly monomers after room temperature digestion with chymotrypsin for 15 min (Figure 10A). Upon further digestion, up to 2 h, only monomer products were detected (data not shown). These products are very nearly the same size as the original GH5 monomers.

It is striking that such a significant fraction of dimer-sized GH5 complexes were reduced to monomer-sized peptides, and this suggests that the two GH5 molecules that cross-linked together on the 22 bp oligonucleotide interacted largely via a single interaction surface in a head-to-tail fashion (Figure 10B). This is in contrast to nonspecific interaction that would have resulted largely in peptides close in size to dimers, and small fragments (Figure 10B). Perhaps indirectly, these results argue that GH5 assembles onto DNA in an organized fashion, though the type of complex or filament remains to be elucidated.

DISCUSSION

A number of previous studies have indicated that linker histones and their globular domains have a tendency to self-associate (15, 40), especially when they are bound to DNA templates (19, 20). However, there has been controversy about whether self-association also occurs in solution, and whether the process is of a specific nature. This research establishes unequivocally that GH5, as well as H5, can undergo self-association in solution, as demonstrated by both turbidity and cross-linking studies. Turbidity is very sensitive to the formation of very large aggregates, which appear in high salt concentrations, and can detect small amounts of such aggregates. Chemical cross-linking is useful in the detection of weak or transient contacts whether they occur in solution or on a DNA substrate, since it is essentially a nonequilibrium process.

For GH5 and H5, DSP cross-linking free in solution resulted in the formation of a broad spectrum of polymers, including some aggregate complexes too large to enter the SDS-polyacrylamide stacking gel. The molar distribution of cross-linked GH5 polymers is indicative of filament assembly via two surfaces, and argues for specificity in the assembly process as originally proposed by Maman et al. (15). Interestingly, the GH5 crystal lattice offers a possible model in which GH5 molecules make contact between the C-terminal end of the protein and the third α -helix (Figure 11). While speculative, this divalent filamentous model appears also to meet the criteria set by the results of quantitative proteolysis that support protein-protein contacts through the C terminus (see below).

DSP cross-linking results indicate that GH5 molecules self-associate more readily when they are bound to linear DNA than when they are bound to supercoiled DNA. Additionally, GH5-linear DNA oligomerization and aggregation appear to have played a major part in the relatively high cross-linking rate. In support of this conclusion, GH5 rapidly self-cross-linked into massive aggregates in the presence of the 42 bp oligonucleotide. Protein oligomers included sizes that extend to the well, and were far too large to have been formed on an individual DNA fragment. In effect, extensive cross-linking could only be indicative of contacts made between separate GH5-DNA complexes.

Supercoiled DNA is distinctly different from linear DNA as a binding substrate for linker histones. Particularly intriguing was the finding that GH5 cross-linked onto supercoiled DNA as clusters, up to three histone molecules in size. A possible explanation is that GH5 binds at DNA crossover in a spatially separated manner in small groups up to trimers. Crossovers appear to act as high-affinity sites for linker histones (47-49) with the globular domain apparently recognizing these DNA structures (52). Interest-

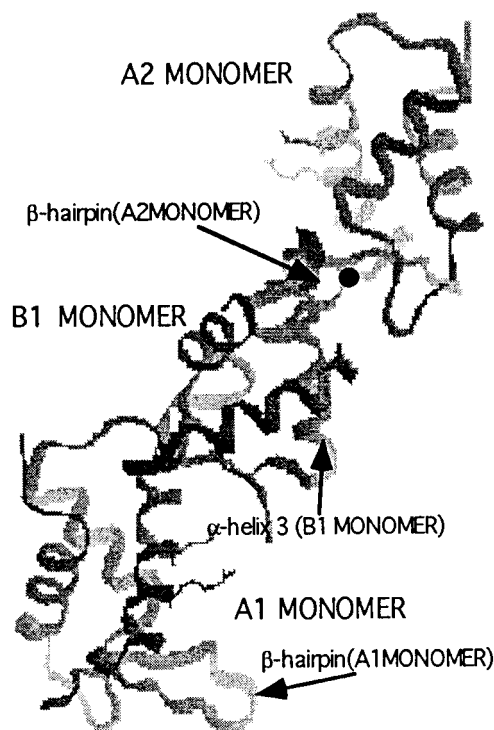


FIGURE 11: Partial GH5 crystal lattice structure based on X-ray diffraction studies by Ramakrishnan et al. (37). Shown are three interacting GH5 proteins that comprise part of a "filament" observed in the crystal; the complete filament consists of two such strands related by 2-fold symmetry. Also identified are the two monomer folding types (A or B) observed in the crystal lattice, and the location of the β -hairpin and the third α -helix. Type A monomers have an extended β -hairpin, while type B monomers contain a β -hairpin that folds back toward the third α -helix. The location of Phe 93 on the A₂ monomer is indicated by a black dot. This computer simulation was generated with InsightII (Biosym, San Diego, CA).

ingly, four-way junction DNA, which may mimic crossovers, can accept three to four GH5 molecules (53, 54), a result that is analogous to and consistent with this GH5 cross-linking study. Crossovers in superhelical DNA may resemble four-way junctions and provide linker histones with a "super affinity substrate". Alternatively, GH5 may not bind at crossover points, but instead, clusters of GH5 may be separated on the DNA by stress-induced structures. For example, EM shows H1 linker histone cooperatively coating isolated portions of a plasmid DNA (50). Separation between H1 clusters appears to be due to stress-related, "bubble-shaped" structures that formed in the plasmid due to H1 binding. However, it should be noted that these experiments used the intact protein, rather than the globular domain. Ultimately, a high-resolution imaging technique may be required to determine whether in fact GH5 binds in small clusters at crossover points.

In a related study, the effects of the protein:DNA ratio and salt concentration on GH5 assembly onto linear DNA were examined. Cross-linking results demonstrate that protein concentration (from 10 to 140% GH5:DNA w/w) had relatively little effect on the overall distribution of GH5 cross-linked polymers. This finding may be consistent with previously reported EM (and sucrose gradient studies) in which the general structure of cooperative GH5–DNA complexes changes little with increasing protein concentrations above 10% GH5:DNA (w/w) (20). GH5–DNA cross-

linking produced results similar to those for H5 (41). The relative distributions of cross-linked H5 complexes were reported to be independent of the H5:DNA ratio, which according to Clark and Thomas (41) is indicative of cooperative binding. However, these authors also report that the H5 cross-linked polymer distribution was independent of the NaCl concentration; we instead found that GH5 cross-linking was highly sensitive to the NaCl concentration. The results appear to be consistent with previous reports of increased linker histone–DNA aggregation with increasing salt concentrations (26, 42, 46).

Finally, quantitative proteolysis was used to elucidate whether GH5 cross-linked onto DNA in a specific manner. GH5 cross-linked and then chymotrypsin-cleaved on a 22 bp oligonucleotide produced results expected for specific contacts. It seems likely that this contact involved the C-terminal region of GH5, since Lys 97 is a good candidate for a cross-linking site which would allow the cross-linked dimer to be reduced to monomer-sized fragments by proteolysis at residue Phe 93. The identification of specific contacts between GH5 molecules bound to DNA suggests that the same surfaces responsible for GH5 self-interactions on DNA may facilitate the self-association of GH5 free in solution.

Linker histone self-association may also have relevance to chromatin fiber compaction. It has been recognized for some time that linker histones H5 and H1 can be extensively chemically cross-linked within the chromatin fiber in situ (54), although cross-linking of the globular domain in situ is reported to be limited to aggregates up to the size of trimers (55). Steric problems associated with nucleosome binding may be partially responsible for the difference, for while the globular domain is securely isolated on the nucleosome, the long linker histone tails are free to interact beyond the nucleosome. In a possibly related observation, nucleosomes reconstituted with linker histones were found to associate and form structures that resemble chromatin (17, 18). This suggests that linker histone tails are capable of bridging separate nucleosomes, with this "bridging" mechanism being potentially important in chromatin compaction and stability. On the basis of the finding that the contacts may be specific, it appears that part of H5-dependent aggregation of nucleosomes may include preferred protein–protein interactions. In summary, the finding that H5 self-interacts with a relatively high affinity is particularly important because it helps explain in situ cross-linking results, and offers a possible explanation for linker histone-induced chromatin stability.

ACKNOWLEDGMENT

We thank Dr. Venki Ramakrishnan for the generous donation of the plasmid GH5pLK, Woojin An for pUC19, and Emily Ray for donating the 42 bp oligonucleotide. Oligonucleotides were synthesized by the Center for Gene Research and Biotechnology (Oregon State University, Corvallis, OR).

REFERENCES

1. van Holde, K. E. (1989) *Chromatin*, Springer-Verlag, New York.
2. Bates, L. D., and Thomas, J. O. (1981) *Nucleic Acids Res.* 9, 5883–5894.

3. Noll, M., and Kornberg, R. D. (1977) *J. Mol. Biol.* 109, 393–404.
4. Allan, J., Hartman, P. G., Crane-Robinson, C., and Aviles, F. X. (1980) *Nature* 288, 675–679.
5. Pruss, D., Bartholomew, B., Persinger, J., Hayes, J., Arents, G., Moudrianakis, E. N., and Wolffe, A. P. (1996) *Science* 274, 614–617.
6. Olins, A. L., and Olins, D. E. (1974) *Science* 183, 330–332.
7. Finch, J. T., and Klug, A. (1976) *Proc. Natl. Acad. Sci. U.S.A.* 73, 1897–1901.
8. Widom, J. (1989) *Annu. Rev. Biophys. Biophys. Chem.* 18, 365–395.
9. Leuba, S. H., Yang, G., Robert, C., Samori, B., van Holde, K., Zlatanova, J., and Bustamante, C. (1994) *Proc. Natl. Acad. Sci. U.S.A.* 91, 11621–11625.
10. Zlatanova, J., and van Holde, K. E. (1995) *J. Biol. Chem.* 270, 8373–8376.
11. Thoma, F., and Koller, T. (1977) *Cell* 12, 101–107.
12. Thoma, F., Koller, T., and Klug, A. (1979) *J. Cell Biol.* 83, 403–427.
13. Hansen, J. C., Ausio, J., Stanik, V., and van Holde, K. E. (1989) *Biochemistry* 28, 9129–9136.
14. Dubochet, J., and Noll, M. (1978) *Science* 202, 280–286.
15. Maman, J. D., Yager, T. D., and Allan, J. (1994) *Biochemistry* 33, 1300–1310.
16. Segers, A., Muyldermans, S., and Wyns, L. (1991) *J. Biol. Chem.* 266, 1502–1508.
17. Ali, Z., and Singh, N. (1987) *J. Biol. Chem.* 262, 12989–12993.
18. Grau, L. P., Azorin, F., and Subirana, J. A. (1982) *Chromosoma* 87, 437–445.
19. Thomas, J. O., Rees, C., and Finch, J. T. (1992) *Nucleic Acids Res.* 20, 187–194.
20. Draves, P. H., Lowary, P. T., and Widom, J. (1992) *J. Mol. Biol.* 225, 1105–1121.
21. Moffat, B. A., and Studier, F. W. (1986) *J. Mol. Biol.* 189, 113–130.
22. Doenecke, D., and Tonjes, R. (1986) *J. Mol. Biol.* 187, 461–464.
23. Cerf, C., Lippens, G., Muyldermans, S., Segers, A., Ramakrishnan, V., Wodak, S. J., Hallenga, K., and Wyns, L. (1993) *Biochemistry* 32, 11345–11351.
24. Gerchman, S. E., Graziano, V., and Ramakrishnan, V. (1994) *Protein Expression Purif.* 5, 242–251.
25. Aviles, F. J., Chapman, G. E., Kneale, G. G., Crane-Robinson, C., and Bradbury, E. M. (1978) *Eur. J. Biochem.* 88, 363–371.
26. Carter, G. J. (1998) Ph.D. Thesis, Oregon State University, Corvallis, OR.
27. Garcia-Ramirez, M., Leuba, S. H., and Ausio, J. (1990) *Protein Expression Purif.* 1, 40–44.
28. Georgel, P., Demeler, B., Terpening, C., Paule, M. R., and van Holde, K. E. (1993) *J. Biol. Chem.* 268, 1947–1954.
29. Maniatis, T., Fritsch, J. T., and Sambrook, J. (1982) *Molecular Cloning: A Laboratory Manual*, Cold Spring Harbor Laboratory Press, Cold Spring Harbor, NY.
30. Laemmli, U. K. (1970) *Nature* 227, 680–685.
31. Sasse, J., and Gallagher, S. R. (1991) *Current Protocols in Molecular Biology*, pp 10.6.1–10.6.8, CRC Press, Boca Raton, FL.
32. O'Neill, R. R., Mitchell, L. G., Merrill, C. R., and Rasband, W. S. (1989) *Appl. Theor. Electrophor.* 1, 163–167.
33. Hill, C. S., Martin, S. R., and Thomas, J. O. (1989) *EMBO J.* 8, 2591–2599.
34. Clark, D. J., Hill, C. S., Martin, S. R., and Thomas, J. O. (1988) *EMBO J.* 7, 69–75.
35. Bohm, L., and Creemers, P. C. (1993) *Biochim. Biophys. Acta* 1202, 230–234.
36. Clore, G. M., Gronenborn, A. M., Nigles, M., Sukumaran, D. K., and Zarbock, J. (1987) *EMBO J.* 6, 1833–1842.
37. Ramakrishnan, V., Finch, J. T., Graziano, V., Lee, P. L., and Sweet, R. M. (1993) *Nature* 362, 219–223.
38. Matthews, H. R., and Bradbury, E. M. (1978) *Exp. Cell Res.* 111, 343–351.
39. Glotov, B. O., Nikolaev, L. G., and Severin, E. S. (1978) *Nucleic Acids Res.* 7, 2587–2605.
40. Russo, E., Giancotti, V., Crane-Robinson, C., and Geraci, G. (1983) *Eur. J. Biochem.* 15, 487–493.
41. Clark, D. J., and Thomas, J. O. (1988) *Eur. J. Biochem.* 178, 225–233.
42. Flory, P. J. (1953) *Principles of Polymer Chemistry*, p 319, Cornell University Press, Ithaca, NY.
43. Watanabe, F. (1985) *Nucleic Acids Res.* 14, 3573–3585.
44. Clark, D. J., and Thomas, J. O. (1986) *J. Mol. Biol.* 187, 569–590.
45. Kowalczykowski, S. C., Paul, L. S., Lonberg, N., Newport, J. W., McSwiggen, J. A., and von Hippel, P. H. (1986) *Biochemistry* 25, 1226–1240.
46. Liao, L. W., and Cole, R. D. (1981) *J. Biol. Chem.* 256, 11145–11150.
47. Vogel, T., and Singer, M. (1974) *J. Biol. Chem.* 250, 796–798.
48. Krylov, D., Leuba, S., van Holde, K., and Zlatanova, J. (1993) *Proc. Natl. Acad. Sci. U.S.A.* 90, 5052–5056.
49. Ivanchenko, M., Zlatanova, J., and van Holde, K. (1997) *Biophys. J.* 72, 1388–1395.
50. De Bernardine, W., Losa, R., and Koller, T. (1986) *J. Mol. Biol.* 189, 503–517.
51. Singer, M. F., and Singer, D. S. (1978) *Biochemistry* 17, 2086–2095.
52. Singer, D. S., and Singer, M. F. (1976) *Nucleic Acids Res.* 3, 2531–2547.
53. Varga-Weisz, P., Zlatanova, J., Leuba, S. H., Schroth, G. P., and van Holde, K. (1994) *Proc. Natl. Acad. Sci. U.S.A.* 91, 3525–3529.
54. Goytisolo, F. A., Gerchman, S., Yu, X., Rees, C., Graziano, V., Ramakrishnan, V., and Thomas, J. O. (1996) *EMBO J.* 15, 3421–3429.
55. Chalkley, R., and Hunter, C. (1975) *Proc. Natl. Acad. Sci. U.S.A.* 72, 1304–1308.
56. Nikolaev, L. G., Glotov, B. O., Dashkevich, V. K., Barbashov, S. F., and Severin, E. S. (1983) *Mol. Biol. (Moscow)* 17, 1255–1261.

BI980716V